EXPERIMENTAL INVESTIGATION OF A HIGH-TEMPERATURE PLANE-LINEAR MODULAR INDUCTION PUMP

E. Yu. Anishev, É. Z. Asnovich,
P. G. Goloborod'ko, L. M. Dronnik,
Ya. Ya. Zandart, A. I. Klimenko,
I. Ya. Kagan, A. S. Kulev,
I. A. Liepin'sh, S. Yu. Reutskii,
V. E. Strizhak, and I. M. Tolmach

UDC 621.313.53

The problem of creating powerful sodium MHD pumps with flow rates of up to 20,000 m^3/h and pressure drops of up to 12 kg/cm^2 for use in power blocks (as alternatives to mechanical pumps) has been analyzed in a number of works in recent years, in particular, in [1-6].

A powerful cylindrical induction pump for a flow rate of 3300 m^3/h, a head of 12.9 kg/cm^2, and a working frequency of 20 Hz, developed in the USA (but not tested), is described in [1], its efficiency equals 45%, it has a mass of 52.3 tons, and the winding is cooled with liquid nitrogen.

The results of tests of cylindrical pumps for the following parameters are presented in [2-4]: total flow rate of 8000 and 20,000 m^3/h and pressure drops of 5.1 and 8.75 kg/cm^2.

The indicated enormous flow rates can also be obtained based on the idea of modularity. In this case the assembly for the total flow rate consists of several induction pumps with lower flow rates, connected hydraulically in parallel. Arrangements of cylindrical [3] and flat [5, 6] pumps are possible.

We definitely prefer the variant consisting of flat pump modules, since in this scheme it is easier to solve the problem of strength of the larger channels and the problem of cooling the windings, and the winding sections are shorter, which also provides a comparatively simple solution to the problem of channeling the inductors without depressurization of the duct.

In order to increase the safety and simplify the operation of such pumps it is desirable to operate them without an external cooling agent (water, nitrogen). In this case the cooling agent for the pump inductors is the pumped liquid metal itself, whose temperature is quite high (300-380°C). The temperature of the inductor winding in the case when a stationary pressure drop of approximately 170°C is realized will be 470-550°C, i.e., it must be highly heat-resistant [7]. This cooling principle is especially desirable for pumps in the first loop, since they must be positioned there in a deep shaft, lowered into a tank with liquid sodium.

Translated from Magnitnaya Gidrodinamika, No. 4, pp. 77-83, October-December, 1986. Original article submitted August 9, 1984.

0024-998X/86/2204- 0405$12.50

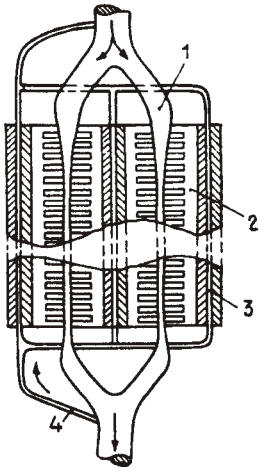

Fig. 1. Schematic diagram of a modular pump of the AMN-6 type. 1) Working channel; 2) inductor; 3) hollow panel on which the inductor is mounted; 4) diversion of an insignificant part of the working flow into the hollow panels.

In developing such a natural pumping setup, weighing tens of tons, it is useful first to develop and test smaller pumps, which, however, are designed based on the same basic principles of the full-scale systems.

In this work, based on what was said above, we investigate a relatively small model of a modular pump of the AMN-6 type, the linear dimensions of whose modules are scaled in the ratio of 1:3 to the modules of a possible full-scale pumping setup. The main characteristics of the model studied are as follows.

1. Modularity. The hydraulic part of the sample consists of two identical flat channels with bilateral inductors, operating in parallel in the common loop.

2. The presence of heat-resistant electrical insulation. The pump inductors are cooled with liquid metal, and in addition there are no external cooling agents, such as water and nitrogen. Aside from the flow of heat into the liquid metal, the channels are equipped for removing heat from the windings into the metal, flowing into special cooling panels. The panels consist of flat channels, adjoining the iron in the inductors on the back side, connected with one another into a parallel hydraulic grid and taking up less than 0.5% of the flow developed by the pump.

3. An autonomous power source – a collection of machines with a synchronous generator with a frequency of 148 Hz. The collection of machines provides the required rundown of the flow of liquid metal when the grid voltage vanishes owing to inertia masses, while the selection of an elevated frequency enables pump operation with magnetic Reynolds numbers from 3-4 (during startup) up to 0.9 (nominal regime), which is close to the values in full-scale setups.

4. The use of an active converging nozzle at the inlet into the channel in order to allow low-pressure operation at the inlet (about 0.5 kg/cm^2).

Description of the Construction. The nominal working parameters of the AMN-6 pump are as follows: the total nominal flow rate Q = 291 m^3/h (80.7 liters/sec), the pressure head developed equals 4 kg/cm^2, the pumped working body is sodium with a temperature of 380°C, and the power extracted from the grid (for the entire pump) equals 123.5 kW. The power factor cos ϕ = 0.32, and the total efficiency equals 25%. The nominal working temperature of the winding equals 510°C, the current load per unit length equals 706 A/cm, the inductor windings are connected in parallel, the line voltage equals 580 V, and the mass of the pump equals 1.6 tons.

Figure 1 shows a schematic diagram of the AMN-6 pump. Structurally the pump consists of two channels placed between three inductors (one inductor is bilateral and two inductors are unilateral). The channel (exterior) is 197 mm wide, the thickness of one wall of the channel equals 2 mm, and the material is Kh18N10T steel. In order to stabilize the flow each channel is separated by barriers 1.2 mm thick into eight identical subchannels. The gap along the liquid metal in the active zone is 13.7 mm wide, the gap at the inlet into the active converging nozzle is 23.7 mm wide. The active zone of each inductor is 1007 mm long, the size of a pole division equals 83.5 mm, and, E330 sheet steel 0.5 mm thick is used for the magnetic circuits of the inductor. The insulation of the winding consists of a) mica

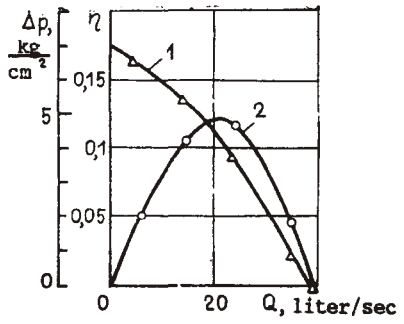

Fig. 2

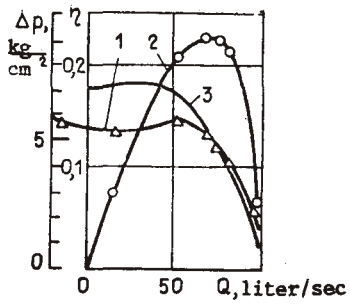

Fig. 3

Fig. 2. Head-flow-rate characteristic (1) and the dependence of the efficiency on the flow rate (2) for a frequency of 50 Hz. The phase current of one inductor is everywhere equal to about 98 A.

Fig. 3. Head-flow-rate characteristic and the dependence of the efficiency on the flow rate for a frequency of 148 Hz. 1) Experimental characteristic; 2) efficiency versus the flow rate; 3) working characteristic. Comparison of calculation with experiment with the phase current of one inductor equal to 92 A.

ribbon (high-temperature) 0.08 mm for the loops and b) molded material from the All-Union Scientific-Research Institute of Electronic Inductive Machines based on fluorophlogopite for the housing [7]. The total thickness of the housing insulation equals about 0.9 mm. Tests of full-scale sections with such insulation, showing that at a temperature of 550°C the breakdown voltage of the housing insulation is about 3000 V while the nominal voltage equals 580 V, were performed beforehand.

The calculation, design, preparation, and testing of no-load operation of the pump were carried out at G. M. Krzhizhanovskii Power Institute. Hot tests were performed at the Institute of Physics of the Latvian SSR Academy of Sciences on the Du-100 liquid-metal loop.

The purpose of the tests was to compare the computed and experimental energy and local parameters, thermal regimes, and strength indicators at the working temperature of the winding, and also to study the transient processes accompanying a change in the power supply to the pump.

No-Load Test. Before the pump was fitted into the loop, tests of ideal no-load operation [8], in which the magnetic field distribution in the gap was measured and the total losses in the steel and walls of the channel were determined for different values of the voltage at frequencies of 50 and 148 Hz, were performed. The losses were approximated by the dependence $P = gU^2$ and the values of the coefficient g were obtained: g = 0.48 S at 50 Hz and 0.32 S at 148 Hz.

The following conclusions can be drawn from the curves of the distribution of the resulting magnetic field in the gap [8]:

1. The spectrum of forward traveling waves contains a peak at the fundamental harmonic. Aside from it, however, there are also quite significant harmonics traveling in the forward direction with both high and low velocities.

2. The amplitudes of the backward traveling waves do not exceed 3% of the amplitude of the resulting field.

3. The field near the edges of the inductor (along its length) decays. The measurements also showed that the field is uniformly distributed over the width of the channel.

Flow Tests. Flow tests of the pump channels were carried out on the Du-100 loop with the windings of the inductors disconnected from the grid. The pressure was increased by smoothly increasing the voltage on the loop pump. The pressure at the inlet and outlet of each channel, the total flow rate (Venturi tube) and the flow rates in each channel were also measured simultaneously with the total pressure drop. The results of the measurements

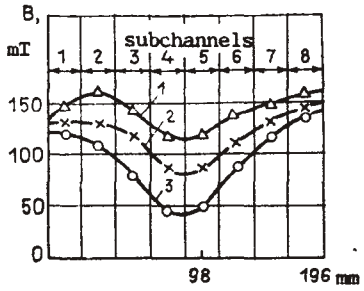

Fig. 4

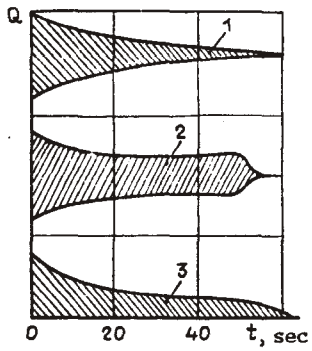

Fig. 5

Fig. 4. Distribution of the induction over the width of the channel. 1) Pump regime, v_{av} = 14 m/sec; 2) pump regime, v_{av} = 8.4 m/sec; 3) stagnation regime, v_{av} = −3.3 m/sec.

Fig. 5. Transient process of pump rundown after the drive motor of the unit is disconnected from the grid. 1) Phase voltage (initial value 230 V); 2) phase current of one inductor (initial value 72 A); 3) flow rate through one channel (initial value 32 liters/sec).

showed that the total coefficient of hydraulic resistance of the pump channels $\xi = \Delta p/Q^2$ equals $2 \cdot 10^7$ N·sec²/m⁸, while for the panels it equals $7.3 \cdot 10^{11}$ N·sec²/m⁸.

Tests Under Working Conditions. Hot tests of the pump were carried out in several stages with successive intensification of the regimes. At the first stage the head-flow-rate characteristics were measured at a frequency of 50 Hz for fixed values of the phase current (62, 78, and 92 A) and a sodium temperature of 250°C. Power was supplied to the pump from an induction regulator (50 Hz; 900 A; 600 V). The cooling panel channel at this stage was not filled with liquid metal.

The measurement results are presented in Fig. 2 in the form of the p(Q) characteristic and the dependence of the efficiency on the flow rates. It is evident from the graphs that the maximum efficiency, equal to 12%, is obtained with a flow rate of 20 liters/sec and a head of 4.3 kg/cm².

At the second stage of the tests power was supplied to the pump from a unit with a frequency of 148 Hz. As before the cooling panels were not filled with liquid metal.

The p(Q) characteristics are presented in Fig. 3. The figure also shows graphs of the changes in the efficiency for regimes with I_{av} = 92 A. The characteristic dips in the p(Q) characteristics in the zone $1 > s > 0.5$ can be seen. The maximum of the efficiency, equal to 25%, corresponds to a regime with a total flow rate of ∿ 80 liters/sec and a head of 4.8 kg/cm², which is somewhat greater than the theoretical data.

The flow rates in the two channels were distributed practically equally in all regimes. There was no cavitation with a pressure of 0.5 kg/cm² at the inlet and a velocity of 16 m/sec in the channel.

The distribution of the resulting induction over the width of the channel was recorded from the measuring coils lying in the channel. Figure 4 shows graphs of the induction of the resulting field in the transverse section of the channel at a distance of 160 mm from the edge of inductor No. 3, opposite to the converging nozzle. The figure also indicates the average velocities in the regimes studied. It is evident that as the slipping increases and transition to the stagnation regime occurs the nonuniformity of the distribution of the induction over the width increases.

At this stage of the tests a loop oscillograph was connected to a flowmeter and the phase of the pump and the transient process of pump rundown after the drive motor of the unit is disconnected from the grid was recorded (Fig. 5). As is evident from the graph, the decay time of the flow rate equals several tens of seconds, which is sufficient for ensuring normal cooling.

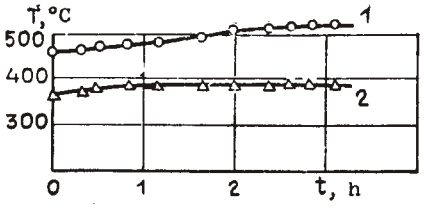

Fig. 6. Curves of the temperature of the winding and of the liquid metal versus the time in the intense thermal regime of the pump. 1) Temperature of the winding; 2) temperature of the liquid metal.

The third stage is the stage of thermal tests with cooling of the inductors to the channels and panels. The p(Q) characteristics were recorded together with the temperature of the inductors and of the liquid metal. The results of the most intense regime with phase currents close to their nominal values (about 92 A) are shown in Fig. 6. The maximum overheating in this regime equaled 128°C. The maximum temperature of the liquid metal equaled 390°C, and the temperature of the winding equaled 518°C, which is close to the theoretical values.

It should be noted here that measures were taken to assure maximum reduction of heat transfer between the windings of the inductors and the external medium, and all of the Joule heat liberated in them was not dissipated, but carried away by the liquid metal.

Comparison of Calculation with Experiment. The method employed for calculation of the induction pumps consists of taking into account the aggregate of all actions of edge effects with the help of coefficients which take into account differently their effect and which follow from the solutions of separate corresponding problems. This makes it possible, by taking into account the main losses of power, to calculate the nominal regimes for a large number of variants. Such an approach was already employed in [14]. We shall list the main factors affecting the motion of the liquid metal in the channel of a flat induction pump:

1) finite width of the channel (transverse edge effect);
2) finite longitudinal dimensions of the inductor (longitudinal edge effect);
3) the finite thickness of the layer of liquid metal (depth effect); and,
4) nonuniformity of the velocity distributions in the transverse section over the width and depth.

The generalized energy expressions, approximately taking into account the combined effect of the indicated factors, are presented below:

$$P_{el}=\frac{1}{2}\sigma v_{av}^2 B_m^2 W\left\{-\frac{s}{1-s}k_{red}k_{red}\frac{k}{k_{bwf}}k_l+c_0-c_t-c_{nu}-c_l\right\};$$

$$P_{em}=\frac{1}{2}\sigma v_{av}^2 B_m^2 W\left\{\frac{s}{(1-s)^2}k_{red}k_{red}k_{bwf}k'_l+c'_l\right\}.$$

Here P_{el} is the electromechanical power, equal to

$$P_{el}=(\Delta p-\Delta p_{fr})Q,$$

where Δp is the pressure drop in the pump, Δp_{fr} is the pressure drop determined by the friction losses; Q is the rate of flow through the pump, P_{em} is the electromagnetic power $P_{em} = P_g - P_c - P_{en+st}$ (P_g is the total power extracted from the grid, P_c and P_{en+st} are the losses in the copper, steel, and envelope of the channel); σ is the conductivity of the liquid metal; v_{av} is the average flow velocity; W is the volume of the channel; B_m is the amplitude of the resulting induction; s is the slipping; k_{red} is the coefficient of reduction of the transverse edge effect, which is found from the analytic solution of the electrodynamic problem, when the flow of conducting liquid in the channel is identical to the motion of a solid conducting strip with the same velocity at all points (the coefficient of reduction according to Vol'dek [9]); k_{redb} permits taking into account approximately the effect of barriers on the coefficient of reduction [10]; the parameter k_{wf} reflects the effect of the hydrodynamics of the flow over the width of a flat channel taking into account the turbulent viscosity and attachment of the flow on the small side faces; the coefficient c_{nu} is a quasiconstant which characterizes the nonuniformity of the velocity profile over the width of the flat channel:

$$k_{wf}=\frac{\bar{k}_{red}}{k_{red}},\quad \bar{k}_{red}=-\int_0^1\frac{\bar{h}_a}{Rm_s}dy,\quad c_{nu}=\int_0^1\frac{\bar{h}_a\Delta v}{Rm(1-s)^2}dy;$$

the coefficients k_{wf} and c_{nu} are studied in detail as a function of the pump parameters in [11]; k_ℓ, k_ℓ' are the coefficients of reduction of the electromechanical and electromagnetic power as a result of the longitudinal edge effect; the coefficients c_ℓ and c_ℓ' are quasiconstants characterizing the shift in the zero value of the electromechanical and electromagnetic power relative to zero slipping owing to the longitudinal edge effect; the coefficients k_ℓ, k_ℓ', c_ℓ, c_ℓ' were determined using the model presented in [12]; and, c_0 is a quasiconstant, reflecting the effect of the nonuniform velocity profile over the depth of the flow [13].

The p(Q) characteristic in a regime close to the nominal regime (the phase current of each inductor equaled 92 A) (see Fig. 3) was calculated using all of the parameters enumerated above.

Comparison shows that the calculation is in satisfactory agreement with experiment and for $s < 0.5$ this agreement is good.

It should be noted that in all of the regimes the friction losses Δp_{fr} were calculated based on the average flow rate through the pump Q using the experimental flow curve. In the region of low average flow rates, with high nonuniformity of the velocity profile, this leads to a too low value of Δp_{fr}. In our opinion this explains the disagreement between the theoretical and experimental characteristics in Fig. 3 for large slippings.

It should be expected that the calculation of friction losses from the local velocity distribution over the width of the channel (and not from the average distribution) will give better agreement over the entire range of slippings.

Conclusion. The tests showed that the construction techniques on which the design of the pump is based, have justified themselves; in particular:

1) modularity – the hydraulic and electromagnetic processes in both channels were virtually identical;

2) active converging nozzles – the flow in all operating states of the pump was of a nonactivated nature, including also with a minimum pressure of 0.5 kg/cm^2 at the inlet;

3) an autonomous power supply enabled normal operation of the pump and rundown over a period of 60 sec in the simulation of an accidental shutdown cooling regime;

4) the cooling panels, together with the channels, enabled effective cooling of the inductors with the liquid metal; the stationary maximum temperature in the head parts of the windings (the hottest location) equalled 518°C in a regime close to a nominal regime with a sodium temperature of 390°C (511 and 380°C theoretically); and,

5) the parameters of the pump were close to the theoretical values, including an efficiency of 26%, indicating the acceptability of the computational method developed.

LITERATURE CITED

1. G. B. Kliman, "Large electromagnetic pumps," Elec. Mach. Electromech., 3, No. 2, 129-142 (1979).
2. I. R. Kirillov, "Electromagnetic pumps for nuclear power," Magn. Gidrodin., No. 3, 87-97 (1982).
3. A. M. Andreev, V. G. Danilin, B. G. Karasev, and I. R. Kirillov, "Selection of construction schemes for electromagnetic pumps for nuclear power plants with fast reactors," Magn. Gidrodin., No. 1, 101-105 (1981).
4. É. Z. Asnovich, E. P. Karelin, A. A. Rineiskii, I. M. Tolmach, A. M. Tuchinskii, and A. I. Él'kin, "Development of high-temperature induction pumps with high flow rate," Magn. Gidrodin., No. 2, 71-78 (1976).
5. L. M. Dronnik, I. M. Tolmach, and A. I. Él'kin, "Problems in the development of electromagnetic pumps for thermonuclear reactors," in: Engineering Problems in Thermonuclear Power Plants [in Russian], Moscow (1981), pp. 11-20.
6. Yu. P. Ushakov et al., "Multichannel induction electromagnetic pump," Inventor's Certificate No. 748749; Otkrytiya, Izobret. Promyshlennye Obraztsy, Tov. Zn., July 17, 1980.
7. E. Z. Asnovich, K. I. Zabyrina, V. A. Kolganova, and B. M. Tareev, Electrical Insulation Materials with High Heat Resistance [in Russian], Énergiya, Moscow (1979).

8. L. M. Dronnik, S. Yu. Reutskii, B. N. Siplivyi, and I. M. Tolmach, "Primary longitudinal effect in flat induction pumps with high flow rates," Magn. Gidrodin., No. 2, 91-97 (1983).
9. A. I. Vol'dek, Induction MHD Machines with Liquid-Metal Working Body [in Russian], Énergiya, Leningrad (1970).
10. I. R. Kirillov, "Induction liquid-metal MHD machine with a spiral channel," Magn. Gidrodin., No. 2, 100-106 (1970).
11. B. B. Volchek, L. M. Dronnik, S. Yu. Reutskii, and I. M. Tolmach, "Transverse edge effect in flat induction pumps with high flow rate," Magn. Gidrodin., No. 4, 93-100 (1981).
12. L. M. Dronnik and S. A. Lifits, "Some mathematical models of a flat induction MHD machine with side busbars," Magn. Gidrodin., No. 3, 113-117 (1983).
13. E. I. Yantovskii and I. M. Tolmach, Magnetohydrodynamic Generators [in Russian], Nauka, Moscow (1972).
14. G. A. Baranov, V. A. Glukhikh, and I. R. Kirillov, Calculation and Design of Induction MHD Machines with a Liquid-Metal Working Body [in Russian], Atomizdat, Moscow (1978).

0024-998X/86/2204- 0411$12.50